

## O-X-B Mode Conversion in the TCV Tokamak

A.Mück<sup>1</sup>, H.P.Laqua<sup>2</sup>, S.Coda<sup>1</sup>, B.P.Duval<sup>1</sup>, T.P.Goodman<sup>1</sup>, I.Klimanov<sup>1</sup>, Y.Martin<sup>1</sup>,  
A.Pochelon<sup>1</sup>, L.Porte<sup>1</sup>

<sup>1</sup> Association EURATOM- Confédération Suisse, EPFL SB CRPP, CH-1015 Lausanne

<sup>2</sup> Max-Planck-Institut für Plasmaphysik, Assoziation EURATOM, D-17491 Greifswald

In high density tokamak plasmas, the accessibility of the plasma to electron cyclotron resonance heating (ECRH) is limited by so-called wave cut-offs. ECRH in extraordinary mode (X-mode) can not propagate to the plasma centre and heating in ordinary mode (O-mode) is prevented by the plasma cut-off at  $\omega = \omega_{pe}$ . At a particular launching angle, an O-mode wave converts to X-mode at the plasma cut-off. After this first mode conversion, the wave propagates back towards the plasma edge until it encounters the upper hybrid layer. There, a second mode conversion from X-wave into a Bernstein (B) wave, known as the O-X-B conversion, occurs. The Bernstein wave can propagate now to the plasma centre and may be absorbed at harmonics of the cyclotron resonance [1],[2].

In TCV, a high density H-mode scenario with up to  $n_e \approx 2 \cdot 10^{20} \text{m}^{-3}$  was developed to place the plasma ECH cut-off within the steep density gradient region at the H-mode discharge edge. The angular window of the O-X conversion is calculated with the power transmission function  $T$  [3]

$$T(N_x, N_z) = \exp \left( -\pi k_0 L \sqrt{\frac{1}{2\alpha}} \cdot \left[ 2 \left( 1 + \frac{1}{\alpha} (N_{z,opt} - N_z)^2 + N_x^2 \right) \right] \right) \quad (1)$$

which depends on the density scale length  $L$  and the refraction indices  $N_x$  and  $N_z$ . Only for the optimum  $N_z$ , equivalent to an optimum angle, can the O-mode wave be completely converted to X-mode.

In figure 1a), the main characteristics of such a H-mode discharge, as used in the reported experiments, is shown. High densities were achieved in non-stationary, but reproducible, discharges. Modulated O-mode ECRH at the second harmonic at 82.7 GHz and  $P_{ECRH} \approx 470$  kW was injected with a low duty cycle to avoid ELM triggering. Poloidal and toroidal ECRH launcher angle scans were then performed on a shot by shot basis. In figure 1b), the change in the stray ECRH radiation signal of a midplane launcher from a diode located in sector 14 is shown. The same tendency in the signal is observed with a second diode in sector 9 and a sniffer probe in sector 2 (ECH is injected from sector 6 of TCV's 16 sectors). A clear dependence on the ECRH launcher angle is observed, shown in further detail in figure 2. In figure 2a) dots show the scan positions for a midplane launcher L4 for the injection angle calculated with the ART code [4]. In the figures 2b) and 2c) the stray radiation signal for the poloidal and toroidal angle scan are drawn separately as a function of the ECRH launcher angle. In these scans, as well as in scans with an upper lateral launcher, the angular dependence of the O-X conversion is clearly visible. The minimum in the stray radiation intensity, assumed to be the maximum of the ECRH power



marked by a solid line. The ART calculated absorption is situated further in the plasma at  $\rho \approx 0.35$  (channels 26, 42).

The calculated position of the plasma cut-off is marked by a dashed line. The ECRH power is reflected at the plasma cut-off and absorbed at the cyclotron resonance after reflection at the torus wall, explaining the correlation outside the cut-off. The amount of ECRH power absorbed is measured with the diamagnetic loop (DML). Figure 4a) shows an average absorbed power of  $267 \text{ kW} \pm 12\%$  (60%) with a phase below  $90^\circ$ , confirming the reliability of the analysis together with figure 4b), which shows that the ECRH modulation frequency was well fitted in the DML signal. If O-X conversion does not take place, the maximum stray level rises to  $S_{\text{stray,max}}$  1.5. In the best case, a stray level of 0.15 is observed, indicating that an O-X coupling of up to 90% was achieved.

The magnetic field dependence of the EBW deposition was investigated by increasing the torio-

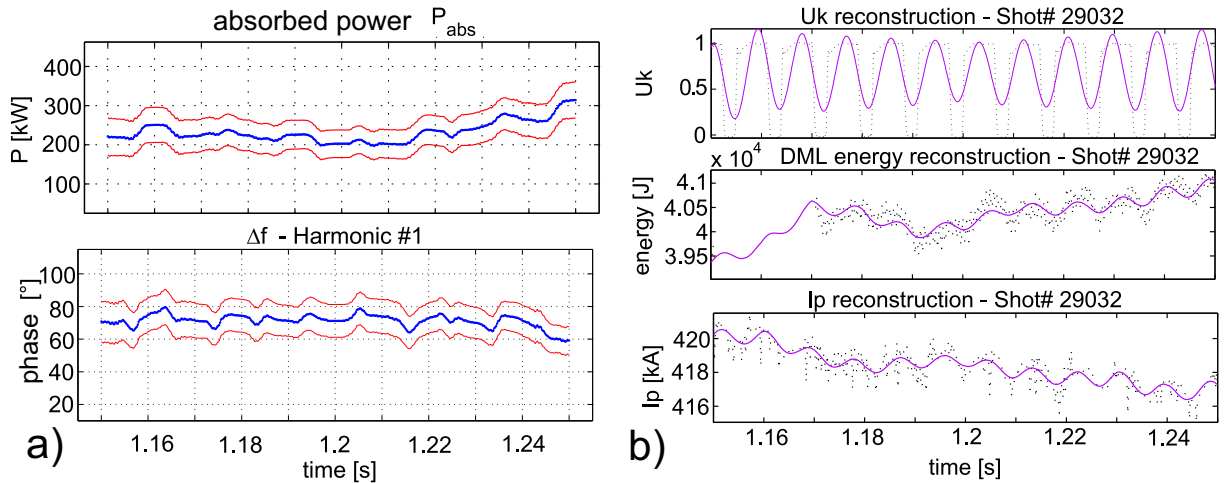


Figure 4: a) Average deposited power and phase with diamagnetic loop. b) Fit of energy and current with ECRH frequency.

dal field from  $B = 1.33 \text{ T}$  to  $B = 1.39 \text{ T}$ . In figures 5a) and 5b) the cross-correlation of  $C_{\text{cross}}$  with the DMPX signal is shown for a sawtooth crash free and ELM free time period. The deposition locations of #29550 and #29565 are consistent with the ART simulation. No significant variation in the deposition location for  $B = 1.33 \text{ T}$  and  $B = 1.39 \text{ T}$  was however observed, as summarised in the table below. A possible explanation could be small changes in the edge current profile, strongly influencing the  $k_{\parallel}$  component of the converted Bernstein wave, leading to a change in

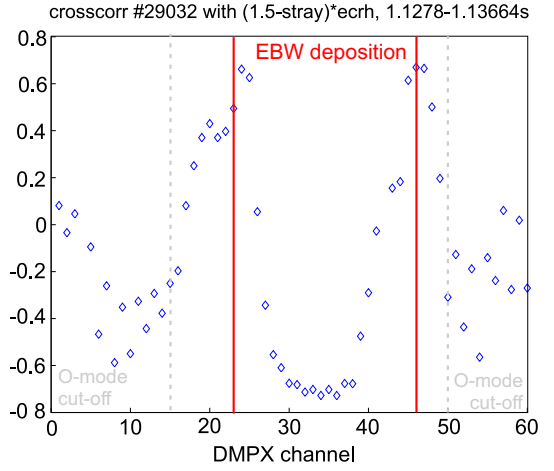


Figure 3: Deposition location of #29032 at  $B = 1.33 \text{ T}$  for ECRH pulse without sawtooth crash.

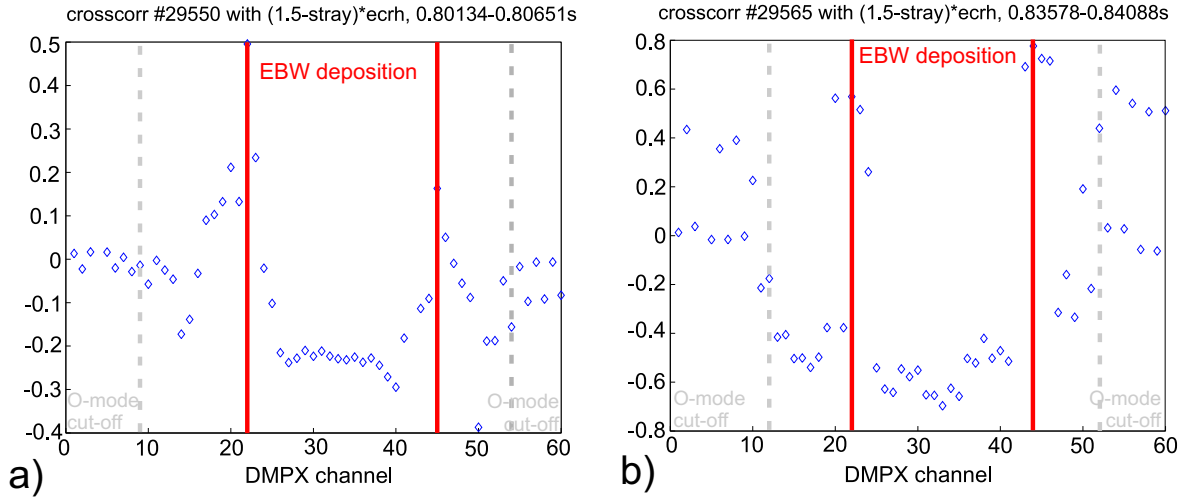


Figure 5: Deposition location of a) #29550 and b) #29565 at  $B = 1.39$  T for ECRH pulse without ELM and sawtooth crash.

the wave propagation. These variations in the current may be in the range of the uncertainty in the equilibrium reconstruction.

Shot	B field	O-X conversion	Absorption (ART)	Absorption (experiment)
#29032	1.33T	$\rho \sim 0.69$ ; ch 15, 50	$\rho \sim 0.35$ ; ch 26, 42	ch 22, 44
#29550	1.39T	$\rho \sim 0.88$ ; ch 9, 54	$\rho \sim 0.45$ ; ch 23, 44	ch 22, 45
#29565	1.39T	$\rho \sim 0.82$ ; ch 12, 54	$\rho \sim 0.45$ ; ch 23, 44	ch 22, 44

### Conclusions:

For the first time in a standard aspect ratio tokamak, localised EBW deposition is demonstrated in overdense plasmas resulting from the O-X-B mode conversion process. Absorption of 60% of the injected ECRH power has been shown by DML measurements in heating experiments. In low power experiments, the stray radiation signal indicates an absorption even up to 90%. The angular dependence of the O-X conversion has been explored by scanning the ECRH launcher angles. The observed variation of the stray radiation signal is well confirmed by ART calculations of the angular window.

### References

- [1] I. Bernstein, Phys. Rev. Lett. **109**, 10 (1958)
- [2] H.P. Laqua et al., Phys. Rev. Lett. **78**, 3467 (1997)
- [3] E. Mjølhus et al., Plasma Phys. **31**, 7 (1984)
- [4] F. Volpe, H.P. Laqua, Rev. Sci. Instrum. **74**, No. 3 (2003), pp. 1409-1413

A. Mück is supported by a EURATOM fellowship.